Optical Engineering

OpticalEngineering.SPIEDigitalLibrary.org

55-in. 8K4K IPS-LCDs with wide viewing angle, high frame frequency, wide color gamut, and stereoscopic

Ryutaro Oke
Junichi Maruyama
Tomohiro Murakoso
Masahiro Ishii
Ikuo Hiyama
Yoshihisa Kato
Hiromasa Yamashita
Kenkichi Tanioka
Toshio Chiba

SPIE.

Ryutaro Oke, Junichi Maruyama, Tomohiro Murakoso, Masahiro Ishii, Ikuo Hiyama, Yoshihisa Kato, Hiromasa Yamashita, Kenkichi Tanioka, Toshio Chiba, "55-in. 8K4K IPS-LCDs with wide viewing angle, high frame frequency, wide color gamut, and stereoscopic," *Opt. Eng.* **57**(7), 075102 (2018), doi: 10.1117/1.OE.57.7.075102.

55-in. 8K4K IPS-LCDs with wide viewing angle, high frame frequency, wide color gamut, and stereoscopic

Ryutaro Oke,[a,*,†] Junichi Maruyama,[a,†] Tomohiro Murakoso,[a] Masahiro Ishii,[a] Ikuo Hiyama,[a] Yoshihisa Kato,[a] Hiromasa Yamashita,[b] Kenkichi Tanioka,[b] and Toshio Chiba[b]
[a]Panasonic Liquid Crystal Display Co., Ltd., Himeji, Japan
[b]Kairos Co., Ltd./Medical Imaging Consortium, Tokyo, Japan

Abstract. We have developed an 8K4K liquid-crystal display (LCD) with diagonal size of 55 inch with the backplane based on an amorphous silicon (a-Si) technology. The 8K4K-LCD has high frame frequency at 120 Hz, which is enabled by a unique technology to compensate the charging voltage of pixels. The achievement of a high resolution of 8K4K including high frame frequency of 120 Hz with a-Si backplanes is ground-breaking for LCDs. Furthermore, a backlight system with laser diode as light source expands the color gamut dramatically. This backlight system enables covering 99% of color space recommended in BT.2020. What is more, the 8K4K-LCD has evolved into a three-dimensional (3-D) display device by attaching a 3-D polarizing film. The vertical viewing angle of the 8K-3D LCD prototype is 8.6 deg at its optimal viewing position set to 1.2 m. [DOI: 10.1117/1.OE.57.7.075102]

Keywords: liquid-crystal display; in-plane switching; 8K; BT.2020; laser diode; three dimensional.

Paper 180502 received Apr. 5, 2018; accepted for publication Jun. 20, 2018; published online Jul. 11, 2018.

1 Introduction

High-resolution displays can provide a strong sense of reality. The resolution in the broadcasting field is worldwide progressing from HD to 4K2K. In Japan, the next broadcasting standard with higher resolution of 8K4K will start in less than a year ahead of other countries. 8K4K is a forceful promotion project of the Japanese Government and NHK Japan Broadcasting Corporation, and it is exactly getting into full swing now.[1] This next-generation broadcasting standard was approved as ITU-R recommendation in 2012, which was standardized as the BT.2020 series in the global broadcast market. BT.2020 series recommended parameter values for ultrahigh-definition television systems for production and international program exchange. The parameter values include not only high resolution of 8K4K but also high frame frequency of 120 Hz and wide color gamut as shown in Table 1.[2] In addition to the next broadcasting system, the field of highly advanced medical treatment expects to make the best use of an 8K4K technology. Medical Imaging Consortium applied an 8K4K imaging technology to clinical trials of a human in 2014.[3] They proved that the detail of an affected area can be well recognized. Moreover, for highly advanced medical treatment, stereoscopic imaging systems with an 8K4K technology are expected for microscopic and endoscopic surgeries because it enables the reduction of accidents such as hurting organs with surgical instruments during surgery.

For now, electronic industry related to an 8K4K technology has been putting effort into the development of mainly broadcasting equipment, such as cameras, recorders, optical transmission, and codecs.[4–7] Recently, the interest has shifted to receiving equipment, i.e., an 8K4K-TV set. To observe the 8K4K-TV set, NHK presents that the observation position to feel a strong sense of reality is 0.75 H (H is the height of a display) from a display, as shown in Fig. 1. In the other parameters, this observation position is equivalent to the field of view (FOV) of 100 deg.

There are two kinds of display devices applied to high-definition TV sets. One is a liquid-crystal display (LCD), and the other is an organic light-emitting diode (OLED) display. OLED displays of the self-emitting device have great advantage of wide viewing angle characteristic in principle. However, OLED-TV sets of 8K4K have a hurdle to overcome and have not yet been mass-produced. It is because the shadow mask required for the manufacturing process of OLED displays for smartphones does not meet the alignment accuracy with a thin-film transistor (TFT) substrate for TVs. Conversely, LCD-TVs of 8K4K with the diagonal size of 70 in. have already gone on sale.[8] Nevertheless, the viewing angle of LCDs is narrower than that of OLED displays. Hence, improvement in the viewing angle is an inevitable theme because of the FOV required for 8K4K-LCDs.

Various kinds of LC modes have been studied from the dawn of LCD research. In particular, representative LC modes are in-plane switching (IPS) and vertical alignment (VA), which are presently applied to mobile phones, PC monitors, TV sets, and so on.[9] The contrast ratio and the color gamut of IPS mode and VA mode are compared in Fig. 2. In spite that the contrast ratio at 0 deg of the VA mode is higher than that of the IPS mode, it steeply drops according to the viewing angle. By contrast, the IPS mode retains up the contrast ratio $>1200:1$ in the FOV range of 100 deg. Additionally, the area of color gamut of the VA mode shrinks and the displayed image appears with a whitish color according to viewing angle. The LC mode in which the characteristics do not change with viewing angle is IPS. As a result, we select the IPS mode as the

*Address all correspondence to: Ryutaro Oke, E-mail: oke.ryuutarou@jp.panasonic.com

†Equally contributed author

Table 1 Parameter values of BT.2020 recommended by ITU-R.

Requirements	Specification
Pixel count	7680×4320, 3840×2160
Frame frequency	120 Hz, 60 Hz
Reference white	(0.313, 0.329)
Primary color/red	(0.708, 0.292)
Primary color/green	(0.170, 0.797)
Primary color/blue	(0.131, 0.046)

technology of a next 8K4K-LCD and the size of 55 in. that is generic and versatile size for TV, broadcasting monitor, and medical monitor.

We presented 55-in. 8K4K IPS-LCD with a high frame frequency of 120 Hz, wide color gamut covering BT.2020, and its stereoscopic technology at SPIE Photonics West 2018.[10] In this journal, we report the details of the technology based on that proceeding.

2 55 Inch 8K4K-Liquid-Crystal Displays Design

2.1 *Pixel Design*

Efficiency for light utilization (transmittance) in LCDs is the most significant feature, which is the strength of LCDs compared with OLED displays. Brightness and power consumption of LCDs are strongly influenced by transmittance. However, improving the performance of LCDs inevitably causes a decrease in transmittance, and there is a trade-off in improving image quality. That is, a decrease in the aperture ratio when the resolution is higher, or a decrease in transmittance of color filter when the color is deeper.

The IPS technology at Panasonic liquid-crystal display (PLD) has evolved on the basis of improvements in transmittance, as shown in Fig. 3. In the beginning when PLD started the development of LCDs, the transmittance of an IPS mode was even lower than that of other LC modes with a view to only a wide viewing angle that was a characteristic of IPS. In 2002, the transmittance of AS-IPS pixel, which had the transparent electrodes for both pixel and common, increased by 30%. After that, we developed the IPS-Pro structure, which improved the contrast ratio.[11–13] The pixel of IPS-Pro has a finger-on-plane, which is composed of transparent finger electrodes on a transparent common electrode plate. The IPS-Pro structure was applied to liquid-crystal panels for TVs for the first time in the world. The transmittance was twice as high as at the start of the development, which realized to take the expensive film that enhances brightness out of the LCD. At last, the IPS-pro-next structure was developed, which improves transmittance dramatically owing to spread the aperture ratio of the pixel.[14] As a result, the transmittance has been enhanced three times as the initial introduction of the IPS technology. Especially, as IPS-pro-next has the advantage of transmittance compared with other liquid-crystal modes when the resolution of LCDs is higher, it became the *de-facto* standard for display devices exceeding 200 ppi such as tablets and smartphones.

The pixel size of an 8K4K panel with the diagonal size of 55 in. is 160 ppi, which is that of the same as a tablet of several years ago. Consequently, it is appropriate to apply IPS-pro-next with shield common electrode to the pixel of the 8K4K panel as shown in Fig. 4. This innovative pixel structure has developed by an evolution from IPS-pro that has production results. The Himeji factory has enough technique to produce high-quality IPS-pro panels. Therefore, we were able to achieve large size panels of 55 in. with the IPS-pro-next structure that had been applied to small high-definition panels.

2.2 *Driving Technology*

2.2.1 *Issue to drive an 8K4K panel*

The key issue of note is that the charge time in a pixel is short because of the 8K4K-LCD-driven 120 Hz. The electric mobility of a-Si TFTs is extremely low, around 0.3 to 0.5 (cm/Vs), which the pixel is charged insufficiently. The most straightforward way to solve this charge shortage is the multiplication of gate-scan so as to double the charge time.

(a) It separates the screen vertically, and drives each screen simultaneously as shown in Fig. 5.

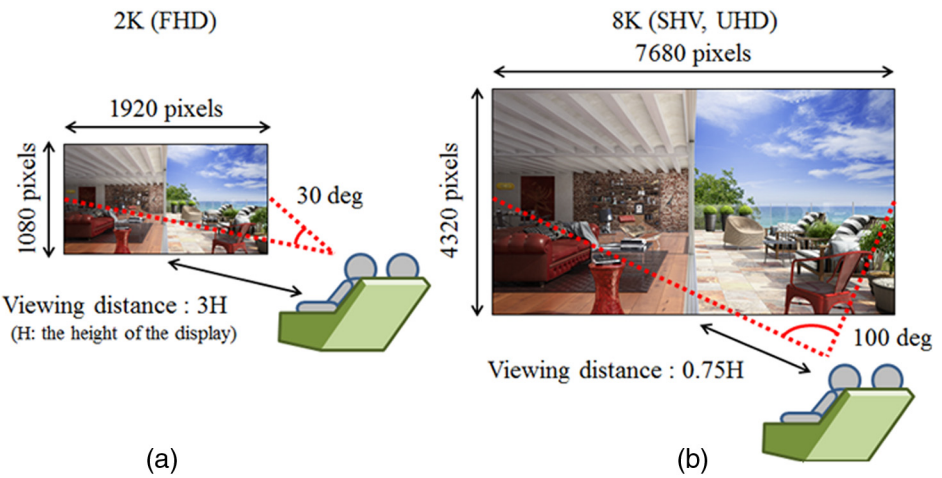

Fig. 1 Comparison of viewing distance (a) 2K resolution and (b) 8K resolution.

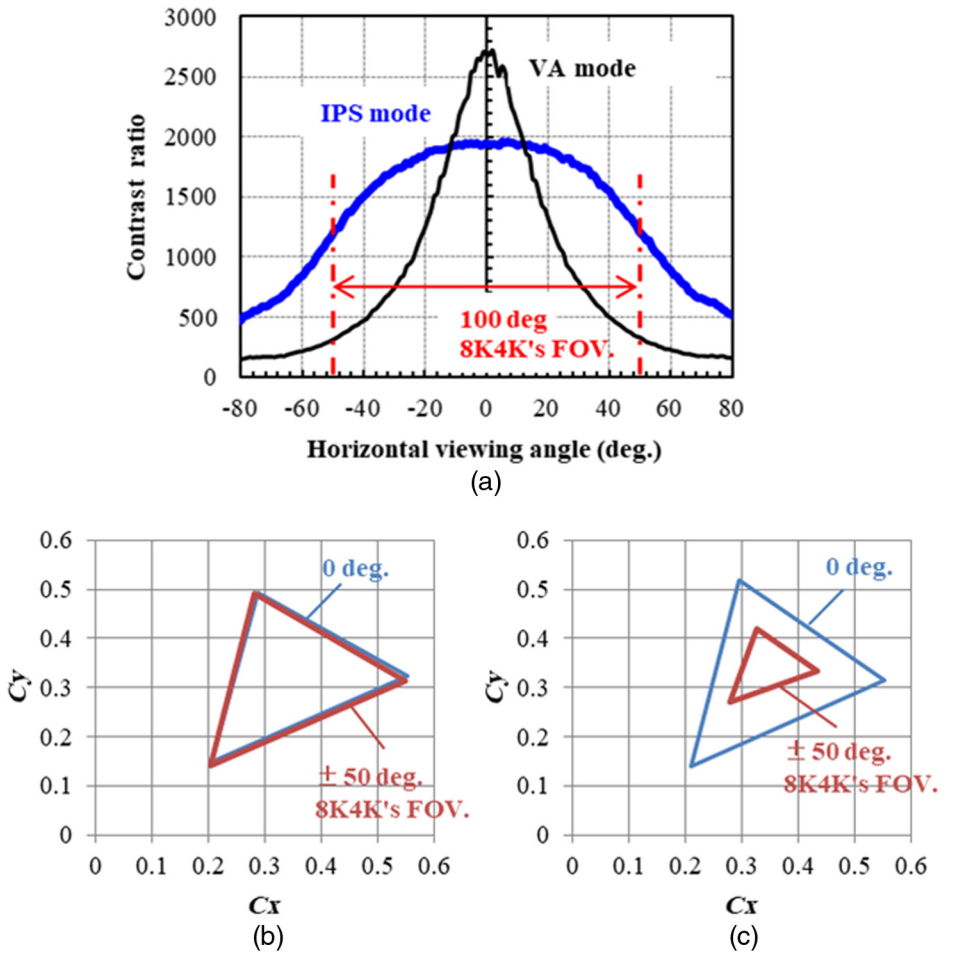

Fig. 2 Viewing angle characteristics of IPS mode and VA mode: (a) comparison of contrast ratio, and comparison of color gamut in the case of (b) IPS mode and (c) VA mode.

(b) It doubles the number of data-line, and drives two consecutive gate lines simultaneously as shown in Fig. 6. This architecture is called 1G2D (1 gate and 2 data) pixel.

1G2D pixel requires twice as much as the data driver required for 1G1D pixel, meaning 96 pieces with a standard data driver that is 960 output pins. Furthermore, with even 1440 output pins, the data-driver requires 64 pieces as well. Thus, it is more difficult to realize a small size panel because 8K4K-LCDs need to mount a lot of drivers. For example, the size of 70 in. or more is required to mount 64 data drivers in a panel as shown in Table 2.

Moreover, 1G2D pixel has a weak point on an aperture ratio in case of high definition because the nontransparent area of wiring metal increases (Fig. 7). As described in Sec. 2.1, there is a trade-off in improving image quality. The loss of transmittance, which is the most important feature of liquid crystal, is one of the issues of 8K4K-LCDs.

In short, 1G2D pixel has some disadvantages, not only the number of drivers mounted, but also the decrease in the aperture ratio. Therefore, these are critical issues for realizing the compact 55-in. 8K4K-LCD. 8K4K-LCDs must be achieved with 1G1D pixel to solve these issues. Adaptive precharge driving (APD) scheme, which is a specific technology of PLD, enables realizing the 1G1D pixel.[15]

2.2.2 *Innovative adaptive precharge driving technology*

In this section, we introduce the principle of APD that improves pixel charging performance. The voltage waveform that charged the data to the pixels in the active matrix driving of LCDs is explained with the pattern displaying the white window on the black background as shown in Fig. 8(a).

The state of driving voltage at a pixel(A) is shown in Fig. 8(b), and the voltage charged to the pixel(A) is insufficient because the time of charging to the pixel in 8K4K-LCDs is too short. Therefore, first, as shown in Fig. 8(c), the time of gate-on is doubled (double gate). As a result, the pixel voltage is sufficiently charged. Charging at the pixel(A) is a best-case condition because of a combination of column inversion driving[16] and double gate. The data voltage is not changed during the period of gate-on owing to display the same white at the previous pixel and the current pixel. Hence, the charging of the pixel(A) is done easily.

By contrast, charging at the pixel(B) is a worst-case condition. In pixel(B), display data are changed from black to white unlike pixel(A). Therefore, there is no effect of double gate lines selection, and the pixel(B) is charged insufficiently as shown in Fig. 8(d). Second, we have proposed a solution to this difficult issue in addition to double gate. As shown in Fig. 8(e), gate-on time is divided into two parts, and

Nick Name (Production Year)	S-TFT ('96)	S-IPS ('98)	AS-IPS ('02)	IPS-Pro I ('04)	IPS-Pro II ('08)	IPS-Pro Next ('11 -)
Products in PLD	•Monitor	•Monitor	•TV (HD) •Monitor	•TV (FHD)	•TV (FHD)	•Tablet •Monitor
Points of Image quality	•Wide viewing angle	•Wide viewing angle (color shift free)	•High transmittance •Wide viewing angle	•High transmittance •High contrast ratio •Wide viewing angle		•High resolution •High transmittance •High contrast ratio •Wide viewing angle
Transmittance	100	100	130	160	200	300
Pixel structure (Plane view)	Metal LC Single domain	Metal Double domain	ITO Transparent electrodes	Two layers ITO TFT lines	Fine pitch ITO	Two layers ITO Lines are shielded
Front view image of a pixel			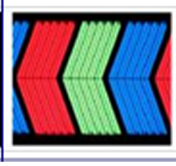	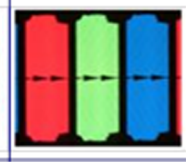	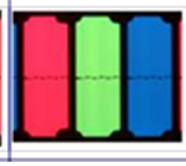	

Fig. 3 Historical development of IPS technology in PLD.

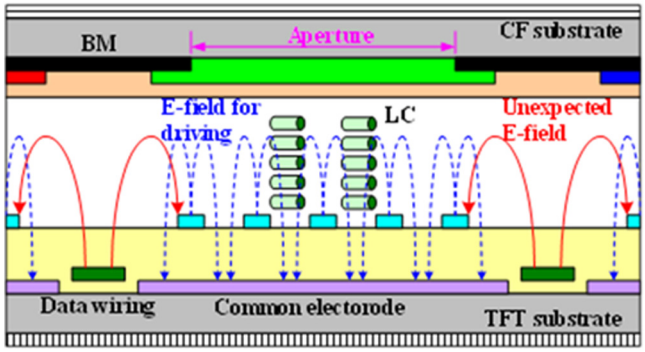

Fig. 4 Comparison of pixel structures (a) without and (b) with a shield common electrode.

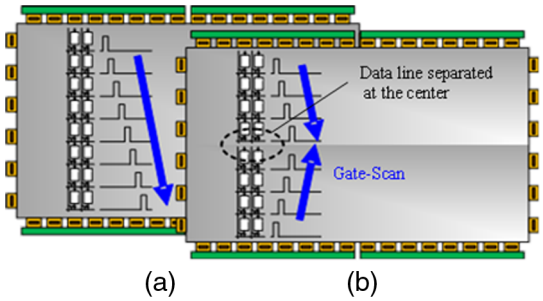

Fig. 5 Schematic panel architecture of the gate-scan method in the liquid-crystal panel: (a) gate single-scan and (b) gate multiscan.

precharged voltage is applied during the former half of the time. The value of the precharged voltage for a combination of all gray-scale levels has been obtained by pixel voltage simulation using SPICE and automatic measurement by 2-D color analyzer (CA-2500).

We applied this APD technology to all of mass production TVs driven at 240 Hz, and it performed adequately with high reliability. However, in terms of improvements desired in conventional APD, there were the following two issues:

(1) The voltage required for precharge is high.

(2) The data driver with the twice of the speed is essential to charge a precharge voltage and a real voltage within a period (1H).

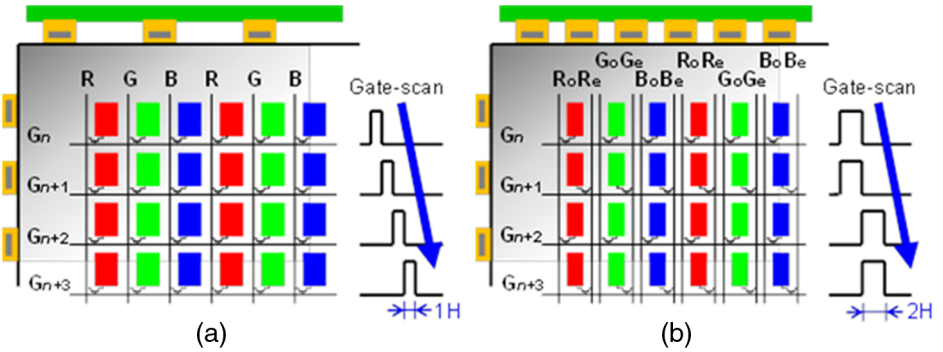

Fig. 6 Relations of the data supply line in case of (a) 1G1D pixel and (b) 1G2D pixel.

Table 2 The number of COF and the panel size which can be equipped with.

Attributes	Units	Specification			
Pixel architecture		1G1D	1G1D	1G2D	1G2D
Channel	Num	960	1440	960	1440
Number	Pcs.	48	32	96	64
Mount limit panel size	inch	45 to 55	30 to 40	80 to 90	70

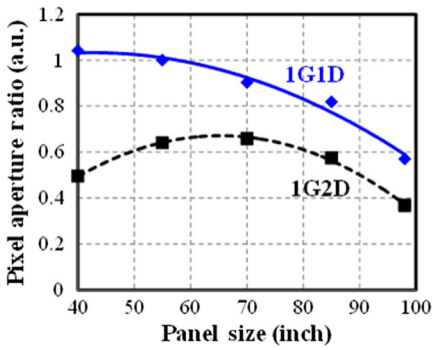

Fig. 7 An aperture ratio loss of the 1G2D structure for the 1G1D structure.

To solve these problems, we propose advanced-APD as shown in Fig. 8(f).[17,18] Inputting an adjusted precharge voltage constantly during 1H period is enabled to reduce a compensation voltage. Moreover, the speed of data does not have to be doubled like conventional APD.

2.2.3 *Simulation result of adaptive precharge driving*

The optimum value of the precharge voltage is determined by charge simulation of the pixel voltage. The simulation tool is based on SmartSpice produced by Silvaco, Inc., and as shown in Fig. 8, the voltage charged to the pixel capacity is calculated by inputting the data voltage through a-Si-TFT of which the model parameters are tuned by ourselves. In the case of pixels optimized for 120 Hz, the size of TFT is too large. Therefore, aperture ratio is reduced and the load of the wiring also increases. Hence, we calculated the precharge voltage to realize 120 Hz with TFT of the comparatively small size optimized at 60 Hz. The ratio of the precharge voltage for the current data voltage in conventional APD is shown in Fig. 9(a). In contrast, Advanced-APD shown in Fig. 9(b) is enabled to make the precharge voltage low as expected. In this graph, data7 shows white data, and data7 shows black data. Precharge ratio (P_{ratio}) is defined as follows:

$$P_{\text{ratio}} = \frac{V_p - V_d}{V_d}, \tag{1}$$

where V_p is the precharge voltage level in the case that the pixel voltage level of Fig. 8(c) is equal to that of Fig. 8(e) or Fig. 8(f), and V_d is the data voltage level in current period of Fig. 8. The precharge ratio was required 26% of white voltage in conventional APD when data changed from black to white. In advanced-APD, we were able to obtain the result that the pixel capacitance was charged enough with precharge ratio of slightly over 13%.

2.2.4 *System architecture of adaptive precharge driving*

The system architecture of advanced-APD is shown in Fig. 10, which is the same as conventional APD. Main components are line memory and look-up-tables. The optimum precharge voltage value is in proportion to difference voltage of the gray-scale levels, an exponential function of a distance from a data driver and the reciprocal of panel temperature, that is, the pre-charge voltage level is given as follows:

$$V_p = V_d + V_{dd} e^{-F(i_{\text{TFT}}, t_H, C_{\text{pix}})} e^{-G(C_d, R_d)}, \tag{2}$$

where V_{dd} is the voltage obtained by subtracting the data voltage of the previous line from that of the current line, i_{TFT} is the TFT-ON current, t_H is the period of 1 H, C_{pix} is the pixel capacitance, C_d is the data-wire capacitance, and R_d is the data-wire resistance. The function F express TFT charging characteristics, and i_{TFT} is related to panel temperature. The function G express electrical time constant of data wire, and R_d is related to a distance from a data driver. All of these data are stored in the electrically erasable programmable read-only memory as a large number of tables.

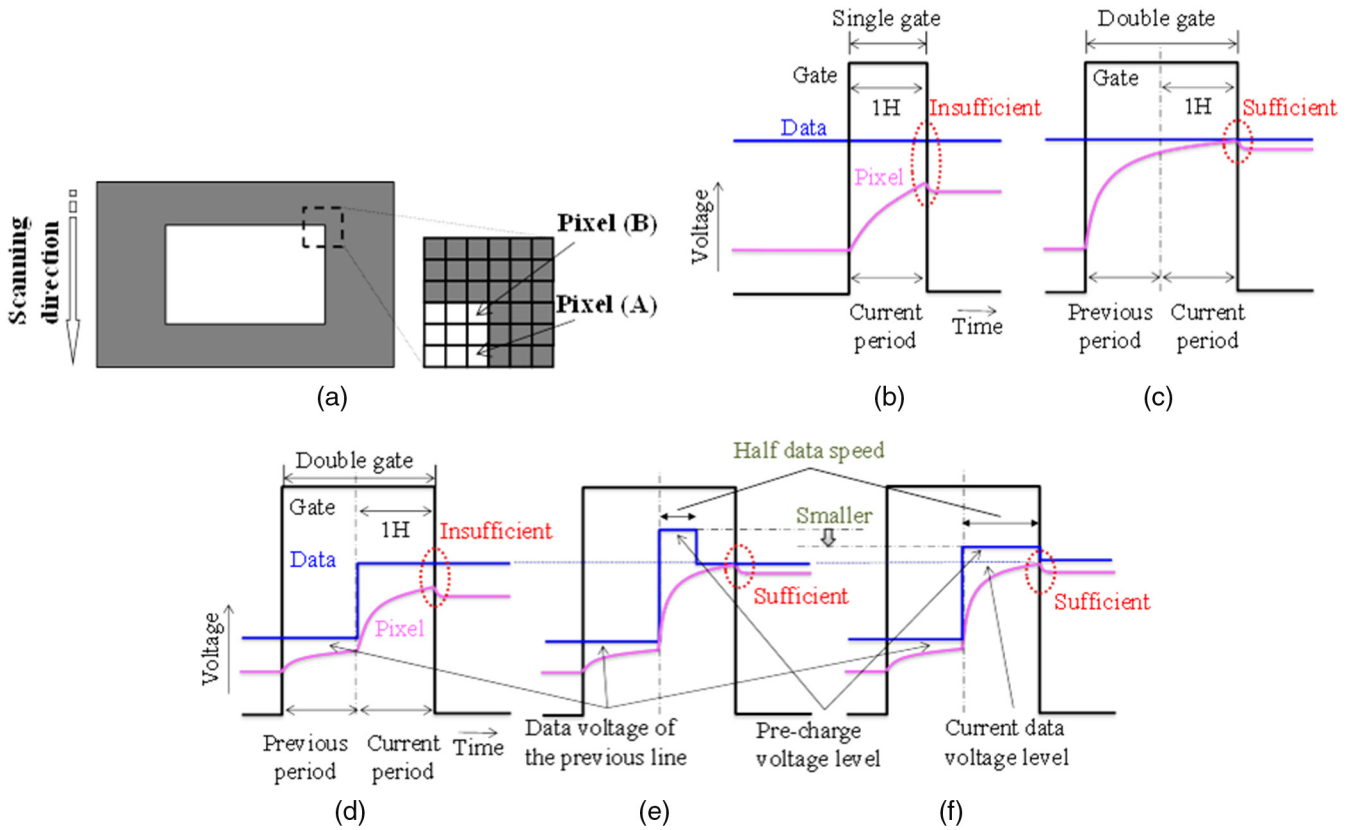

Fig. 8 APD technology compensating the charge shortage of the pixel: (a) display pattern and the position of the pixel to be considered, (b) voltage waveform of a pixel(A) with single gate, (c) voltage waveform of a pixel(A) with double gate, (d) voltage waveform of a pixel(B) without APD, (e) voltage waveform of a pixel(B) with APD, and (f) voltage waveform of a pixel(B) with advanced-APD.

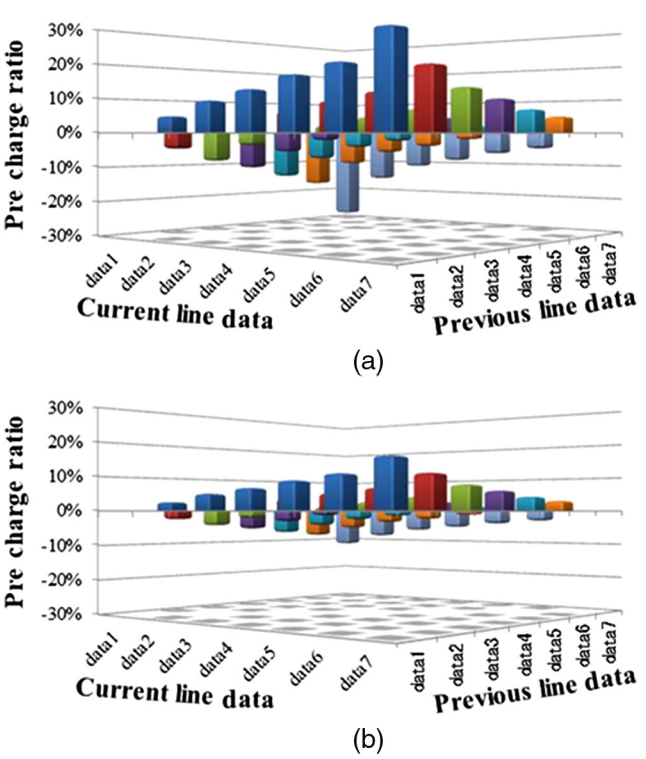

Fig. 9 Precharge ratio (the ratio of the precharge voltage for the current data voltage) comparison between (a) conventional APD and (b) advanced-APD.

2.3 *Wide Color Gamut*

2.3.1 *Color gamut corresponding to the light source*

The benchmark result of color gamut with various light sources toward BT.2020 is shown in Fig. 11 and Table 3.

LCDs have been able to cover Adobe RGB and DCI-P3 with conventional color technologies. The color gamut of LCDs is wider than that of OLED displays owing to functional parts are separated by a light source of backlight and a color filter. Nevertheless, white LEDs based on blue LEDs, which contain the red and green phosphor, cover only about 82% for BT.2020. Because full width at half maximum (FWHM) of the wavelength of the blue LED is as wide as ~55 nm and that of the red and green phosphor are very broad, blue and green, red and green are mixed. Therefore, it is really difficult to widen the color gamut with a combination of the blue LED and the phosphor. FWHM must be <10 nm to fully cover this BT.2020. The wide color gamut technology using quantum dots (QDs) has been the most popular recently. Although the FWHM of QDs with toxic cadmium is as narrow as ~20 nm, that of QDs without cadmium is ~40 nm. In case of this FWHM, QDs can express only colors slightly deeper than LEDs with phosphor. Ultimately, now, to cover almost 100% of BT.2020, we have no choice but to apply laser diodes of three primary colors to a backlight. Each FWHM of laser diodes with three primary colors are 2 nm or less, and each color is reliably split.

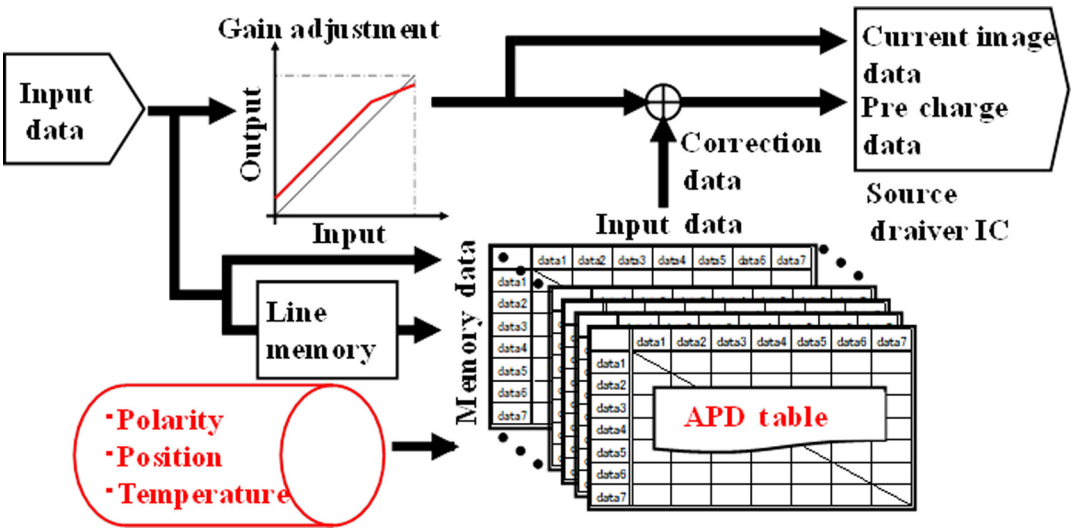

Fig. 10 System architecture of APD.

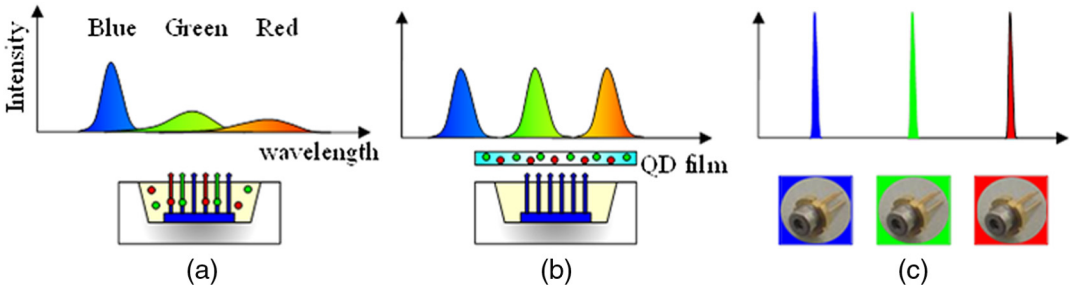

Fig. 11 Various light sources for LCDs and the peak wavelength (a) B-LED + RG-phosphor, (b) B-LED + QDs, and (c) RGB-all-laser.

Table 3 Benchmark results of color gamut ($u'v'$ covering) by representative color technology.

Devicetype	Specification	
Color target	DCI-P3/Adobe RGB	BT.2020
OLED for TVs	85%	65%
LCD with B-LED + RG-phosphor	100%	82%
LCD with B-LED + QDs	100%	87%
LCD with three primary color laser diodes	100%	99%

In this work, we achieved wide color gamut of the 8K4K panel in two stages. First, as a realistic solution, we realized to cover 100% of DCI with a white LED. In the next stage, as a future solution, we realized to cover close to 100% of BT.2020 with laser diodes of three primary colors.

Next, we will explain a laser diode.

2.3.2 *Laser diode to cover BT.2020*

The color gamut of LCDs is flexibly controlled by matching between the spectral luminance of the light source and the spectral transmittance of the color filter. Whereas, in case of a laser diode, the color gamut of LCDs is determined mainly by peak wavelength of the diode because its FWHM is only 2 nm or less. The optimum peak wavelength of laser diode required to cover BT.2020 is 638, 530, and 463 nm for red, green, and blue, respectively. The technology of red and blue laser diodes has been established and is available on the market. However, green laser diodes still have some room for improvements. The output efficiency of a GaN-based laser diode decreases as the wavelength becomes longer. In particular, the efficiency of green lasers is low, which is a major problem for display devices. Nonetheless, the wide color gamut of the three primary color laser diodes is highly expected for display devices other than LCDs. One of them is light sources for a projector. The cost of laser diodes would be expected to go down by applying to projectors and LCDs and growing together.

Hence, in the second stage, we developed a backlight for 55-in. 8K4K-LCDs with three primary color laser diodes that can cover 100% of BT.2020 color gamut.

2.3.3 *Laser diode backlight*

In the case that laser diodes are applied to the backlight of LCDs, another issue is to make surface light sources. Although LED has Lambertian distribution, laser diodes have strong directivity. In the case of LED backlights, the light is directly input to a light-guide-plate as shown in Fig. 12(a). Contrary to this, in the case of laser diode backlights, a

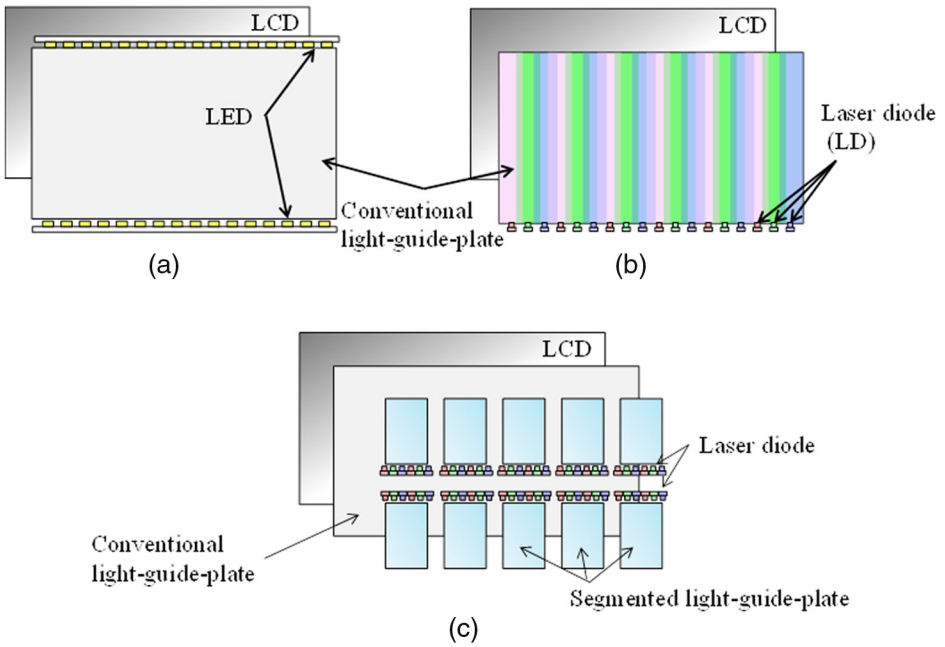

Fig. 12 Backlight structure with laser diodes as the light source (a) LED backlight, (b) laser-diode backlight, and (c) laser-diode backlight with segmented light-guide-plates added.

simple combination of laser diodes and conventional light-guide-plate cannot avoid Mura as shown in Fig. 12(b).

We solved this problem by developing the combination of multiple light-guide-plates as shown in Fig. 12(c). Once the light is diffused by the added segmented light-guide-plates, the diffused light is input to a conventional light-guide-plate from panel edge.

As a result, the luminance uniformity of the backlight with laser diodes can be made equivalent to that of the backlight with LEDs.

2.4 *Effect of Prototype Sample*

We achieved the 55-in. 8K4K prototype sample in the mass production line of 8.5 generations in Himeji. As shown in Fig. 13(a), color shift of IPS mode is not visually recognized at all at the viewing angle of 100 deg. Fig. 13(b) shows a monitor with a VA mode, which is currently sold in the market for comparison purposes. Thus, it changes to whitish colors at the viewing angle of 100 deg.

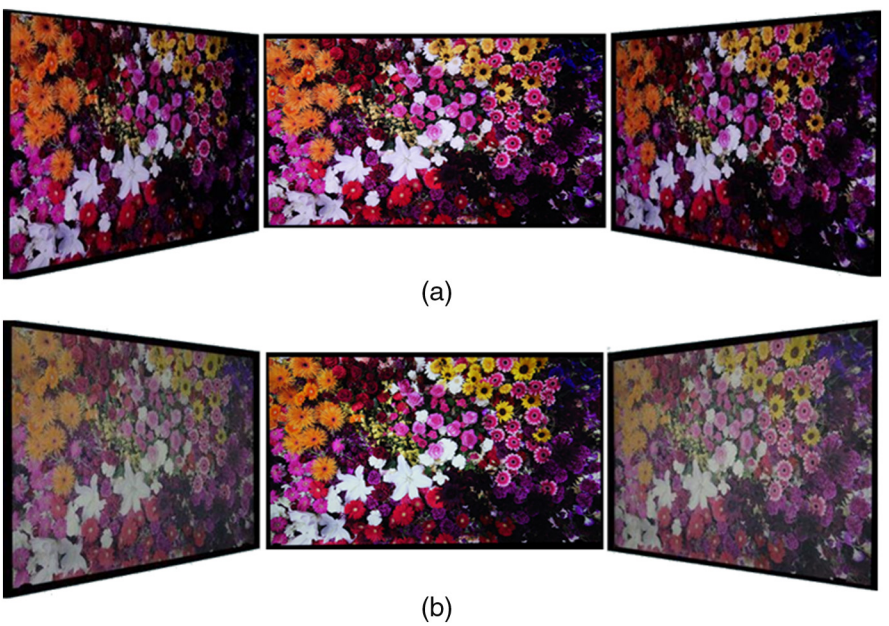

Fig. 13 Viewing angle characteristics in case of (a) IPS mode and (b) VA mode: (Left) 50 deg viewing angle, (center) 0 deg viewing angle, and (right) +50 deg viewing angle.

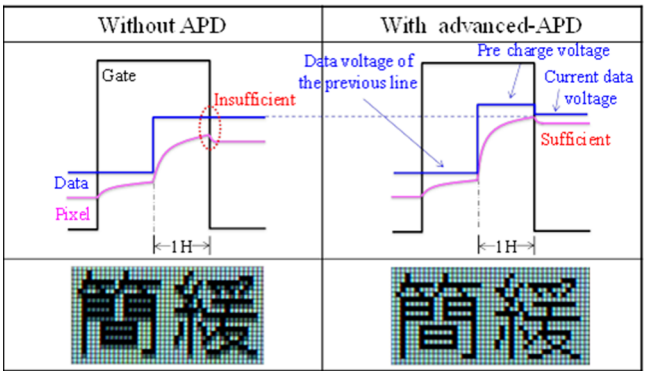

Fig. 14 An example of APD effect.

2.4.1 *Advanced-adaptive precharge driving image quality*

In such a way as to confirm the effectiveness of APD, we compared front view photographs of character image displayed on a 55-in. 8K4K panel driven 120 Hz as shown in Fig. 14. The displayed image is black characters on a gray background with 50% brightness, which makes it easy to recognize the difference visually. Brightness of the gray pixel of the line next to the black pixel on the LCD driven without APD was decreased. Consequently, the characters looked smeared. The pixel of which brightness became dark is definitely caused by the shortage of charging from the pixel TFT.

In contrast, APD was enabled to obtain a clear outline of the character because it fully charged each pixel capacitance in the panel.

It turned out that APD is an innovative technology that has the effect of improving the charging performance of TFT.

2.4.2 *Characteristics of 55-in. 8K4K display*

Characteristics of 55-in. 8K4K display developed this time are shown in Table 4. In the first stage, 400 nit of luminance and 100% of DCI-P3 were achieved, and the power consumption was only 180 W. It is expected to promote the 8K for consumer use. In the second stage, we realized the ultrawide color gamut covering 99% of BT.2020 using a laser diode backlight. In addition to broadcasting and medical use, it is expected for being applied to archives because it can reproduce details and colors of cultural properties.

2.4.3 *Impact*

First, we demonstrated the 8K4K panel of DCI-P3 in CES2015 (Fig. 15). The achievement of an 8K4K panel driven at 120 Hz despite a-Si TFT has made a great impact on many industry officials. In addition, due to its compact size of 55 in., it is expected to develop into various applications.

Next, we demonstrated the 8K-LCD with laser-diode backlight in CES2016 (Fig. 16). A lot of visitors viewed the BT.2020 images, compared with conventional color. They expressed their impressions as follows, "it felt brighter," "it felt like high definition," and "it felt stereoscopic."

Table 4 Specifications of prototype 55-in. IPS-LCD.

Attributes	Units	Specification	
Color target		DCI-P3/Adobe RGB	BT.2020
Display diagonal size	inch	55	55
Native resolution		8K4K 7680 × 4320	8K4K 7680 × 4320
LC alignment process		Photoaligned IPS	Photoaligned IPS
Display colors	bit	10	10
Pixel pitch	mm	0.1575 (160 ppi)	0.1575 (160 ppi)
Data driver count	pcs.	48	48
Luminance	nit	400	350
Contrast ratio		1500:1	1500:1
Picture frame rate	Hz	120	120
Color gamut ($u'v'$ covering)		100% (DCI/Adobe RGB) 82% (BT.2020)	100% (DCI/Adobe RGB) 99% (BT.2020)
Power consumption	W	180	350

Fig. 15 Table type 55-in. display in International CES 2015.

Fig. 16 55-in. 8K4K display realized color gamut covering 99% ($u'v'$) of BT.2020 with the laser diode in International CES2016: we collaborated with the connection technology of plastic optical fiber.[19]

3 Stereoscopic

3.1 *Effect of Three-Dimensional Technology in Medical Field*

Camera and monitoring systems that support surgeon's vision are one of the most promising advanced medical technologies. These systems are an endoscope and a microscope surgery system, and expanding recently. However, accident such as hurting organs with surgical instruments during operations is concerned, and stereoscopic is required in these procedures, as shown in Fig. 17(a). Furthermore, a medical application of 8K4K technology has been enabled to recognize the details of organs. Medical Imaging Consortium succeeded in the world for the first time in clinical application applying 8K4K imaging technology as shown in Fig. 17(b) in 2014.[3] As a result, it was demonstrated that surgeon was able to recognize clearly the details of diseased parts. Moreover, the imaging of 8K4K has wide viewing field, and can prevent the collision of surgical instruments and an endoscope during the operation.

In this section, we describe a stereoscopic technology based on 8K4K IPS-LCDs.

3.2 *Three-Dimensional Display System with a Polarization Filter*

The mechanism of stereoscopic is that a right-eye-image and a left-eye-image are observed by a right eye and a left eye, respectively. In general LCD-TVs, there are two approaches for realizing stereoscopic. One is a frame sequential driving, which is based on a time division of a right-eye-image and a left-eye-image. The other is a 3-D polarization filter on a surface of a LCD, which is based on a space division of those images. It is important for medical applications to reduce fatigue of surgeons. Hence, the space division technique has adopted by surgeons for the reason of some advantages, such as lightweight, flicker-less, and battery-less eyeglasses. However, this technique has two issues as described below.

(1) Reduction of vertical resolution and
(2) Restriction of viewing angle along the vertical direction.

The vertical resolution in 3D-LCDs based on the space division is half of that in 2D-LCDs in essence. Thus, the detail of image is much spoiled in the case that the resolution of LCD is low. Typical images output on a FHD-3D and an 8K-3D display are compared in Fig. 18. Edges of objects on the FHD-3D display are jagged, for this reason, the detail of structure is lost. This is the first issue, "reduction of vertical resolution." By contrast, the 8K-3D display is enabled to avoid severe artifacting of edges of objects.

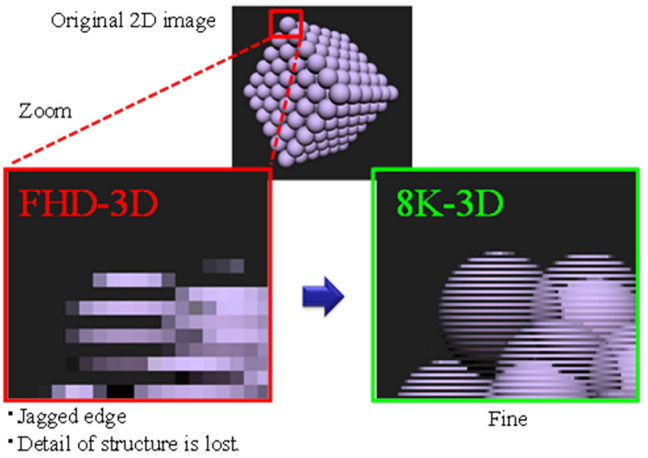

Fig. 18 Comparison of image resolution displayed on the FHD-3D and the 8K-3D.

In the situation that surgeons observe at right in front of a 3-D display, they are able to recognize stereoscopic. However, in the situation that the display is observed from tilted angle in the vertical direction, the left- and right-eye-images are overlaid in eyes of surgeons as shown in Fig. 19. This mixture of each eye's image is known as 3-D crosstalk. In this case, the separated left- and the right-eye-image reach both eyes. This is the second issue, "restriction of viewing angle along the vertical direction."

The cause of occurrence of 3-D crosstalk is shown in Fig. 20. In the situation of observation at right in front of a 3-D display, the light beam from a left-eye-pixel of an LCD reaches the left-eye of the observer through a filter for the left-eye. The light beam of a right-eye-pixel is also the same. Therefore, the observer can recognize 3-D images correctly. In contrast, in the situation of observation at any tilted angle, a part of the light beam from the left-eye-pixel reaches the right-eye of the observer through a filter for the right-eye. The origin of the 3-D crosstalk phenomenon is the mixture of the light beams.

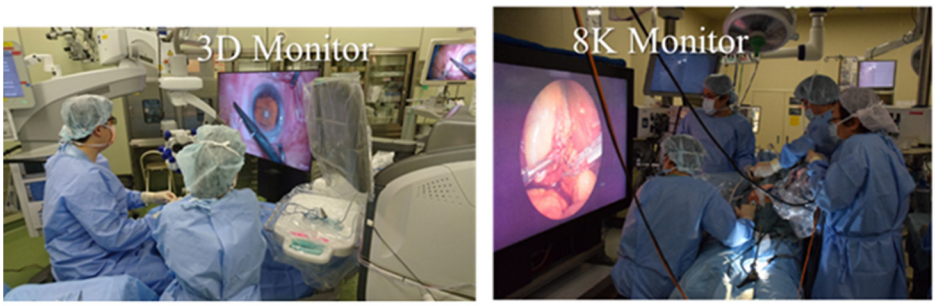

Fig. 17 Cameras and monitors support surgeon's vision: (a) 3-D heads-up surgery for ophthalmology and (b) 8K endoscopic surgery, [Photograph (a) is provided by Takashi Koto, Kyorin University, the department of ophthalmology].

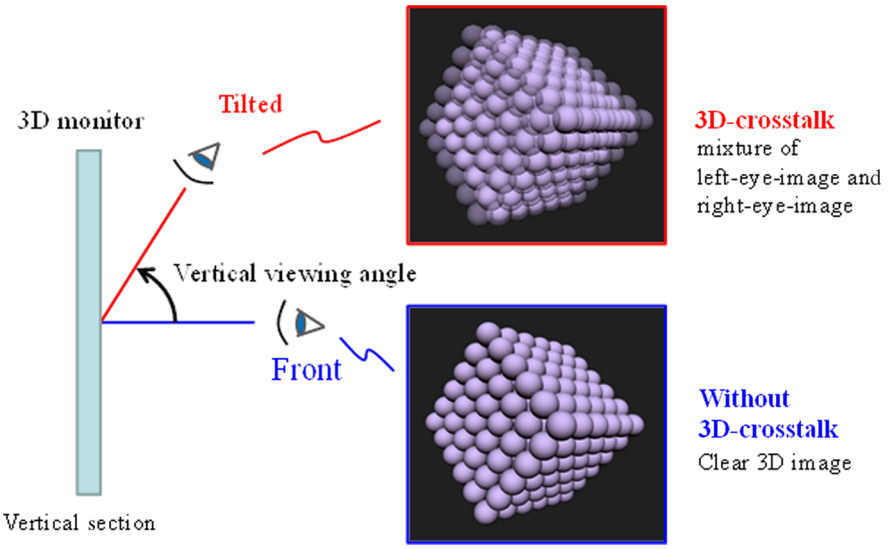

Fig. 19 Limited viewing angle along vertical direction.

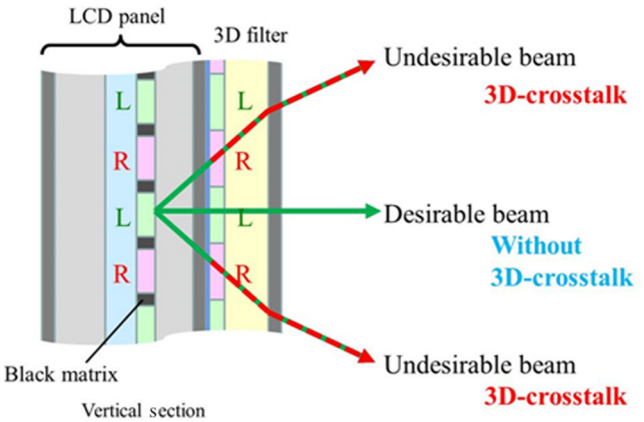

Fig. 20 3-D crosstalk phenomenon.

Meanwhile, the debasement such as reduced resolution and 3-D crosstalk is not observed from the horizontally tilted angle at all. A wide viewing-angle characteristic, which is a merit of IPS-LCDs, can be obtained completely along the horizontal direction.

3.3 *Optimal Viewing Position*

In the stereoscopic based on a space division technique, there are limitations on the position where the whole screen can be observed clearly due to 3-D crosstalk. Furthermore, the advantages of high resolution of 8K4K are not obtained even if the viewing distance is too close or too far away. Thus, the viewing distance from a 3-D monitor need to be decided to design a 3-D filter properly. We decided the distance between a surgeon and an 8K-3D monitor to be 1.0 to 1.5 m, which considered practical examples of 3-D head-up surgery for ophthalmology as shown in Fig. 21(a). In addition, the 3-D monitor is located at 1.0 to 1.5 m apart from the surgeon, such as the layout of the operating room for ophthalmology is shown in Fig. 21(b). This space is required to set an operating table. In general, the defined viewing distance for 8K-2D displays, as described in Sec. 1, is 0.75 times the screen height. In contrast, the optimal viewing distance for 8K-3D displays based on the space division technique is 1.5 times its height due to reducing the vertical resolution by half as shown in Fig. 22.

We drew a conclusion from the studies discussed above that the diagonal-size of 55 in. was suitable for medical 8K-3D.

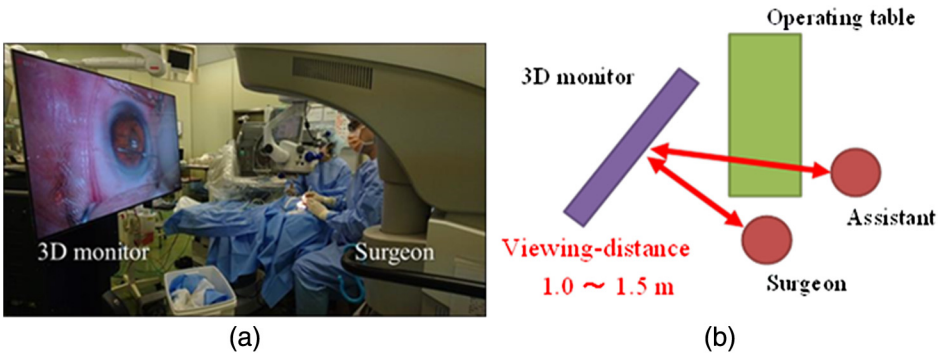

Fig. 21 Viewing distance of 3-D monitor (a) 3-D heads-up surgery for ophthalmology and (b) example of operating room layout (top view), [photograph (a) is provided by Takashi Koto, Kyorin University, the Department of Ophthalmology].

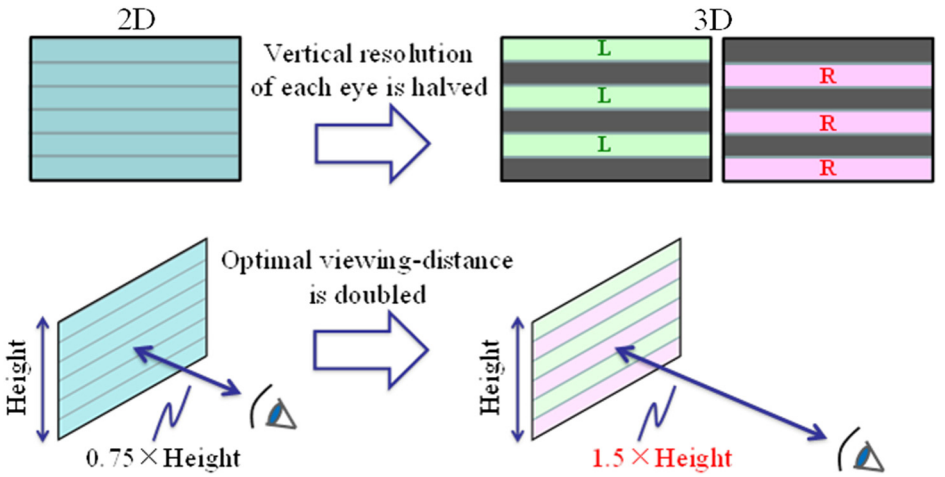

Fig. 22 Optimal viewing distance of 8K.

Table 5 Dimensional parameters for the simulation.

Attributes	Units	Specification
Display diagonal size	inch	55
Resolution		8K4K 7680 × 4320
Pixel pitch	mm	0.1575 (160 ppi)
Black matrix (BM) width	mm	0.0595
Color filter (CF) substrate thickness	mm	0.5
Refractive index of CF glass		1.5
Polarization filter (PF) thickness	mm	0.201
Refractive index of PF		1.5

We simulated the 3-D crosstalk ratio with ray tracing simulation to fabricate the 3-D polarization filter. The mixture ratio of unsuitable beams included in the output beams was expressed by the 3-D crosstalk ratio. The required dimensional parameters for the simulation are shown in Table 5. In this work, some part of the parameters were fixed, and the pitch of a 3-D polarization filter was changed corresponding to various conditions of the viewing distance of 1.0, 1.2, and 1.5 m. The estimated region of stereoscopic is shown in Fig. 23. We set the maximum 3-D crosstalk ratio to 7%.[20] Namely, the position where the 3-D crosstalk ratio is <7% is expressed by the diamond-shaped areas in Fig. 23. Surgeons can recognize clearly stereoscopic image in these areas. The region of stereoscopic vision is 0.8 to 1.3 m, 0.9 to 1.5 m, and 1.2 to 2.5 m, respectively, for the viewing-distance of 1.0, 1.2, and 1.5 m. As a result, we decided the suitable viewing-distance as 1.2 m covering the range of 1.0 to 1.5 m. In this case, the vertical viewing angle was calculated 8.2 deg, and when stereoscopically viewable area is converted to height, it corresponds to ~17 cm. In the case of 3-D heads-up surgery, surgeons and assistants are sitting in a chair and can recognize stereoscopic viewing because the height of the viewpoint is stable. As described in Sec. 3.2, there is no constraint on the 3-D viewing angle

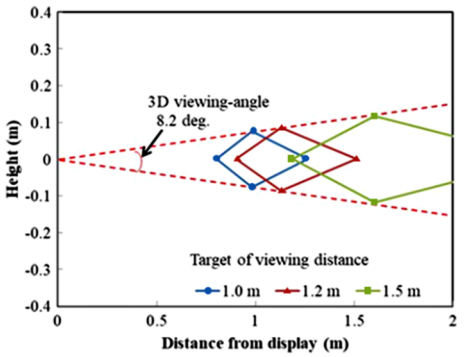

Fig. 23 Estimated region of stereoscopic along vertical direction.

with respect to the horizontal direction. Therefore, stereoscopic viewing is obtained at the same time not only by surgeons, but also by assistants.

We manufactured 8K-3D IPS-LCDs with parameters in Table 5 and the target viewing distance of 1.2 m. The results of measuring 3-D crosstalk are shown in Fig. 24. The vertical viewing angle with the 3-D crosstalk ratio of 7% or less is ~8.6 deg (Fig. 24). The measurement and the simulation of 3-D crosstalk are matched accurately. Thus, we confirmed

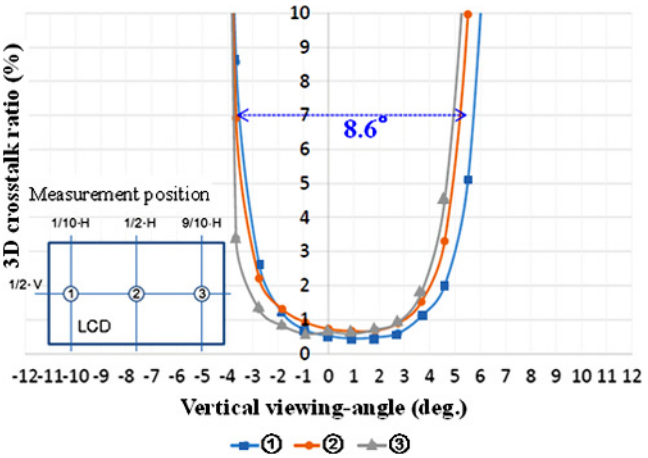

Fig. 24 Results of 3-D crosstalk.

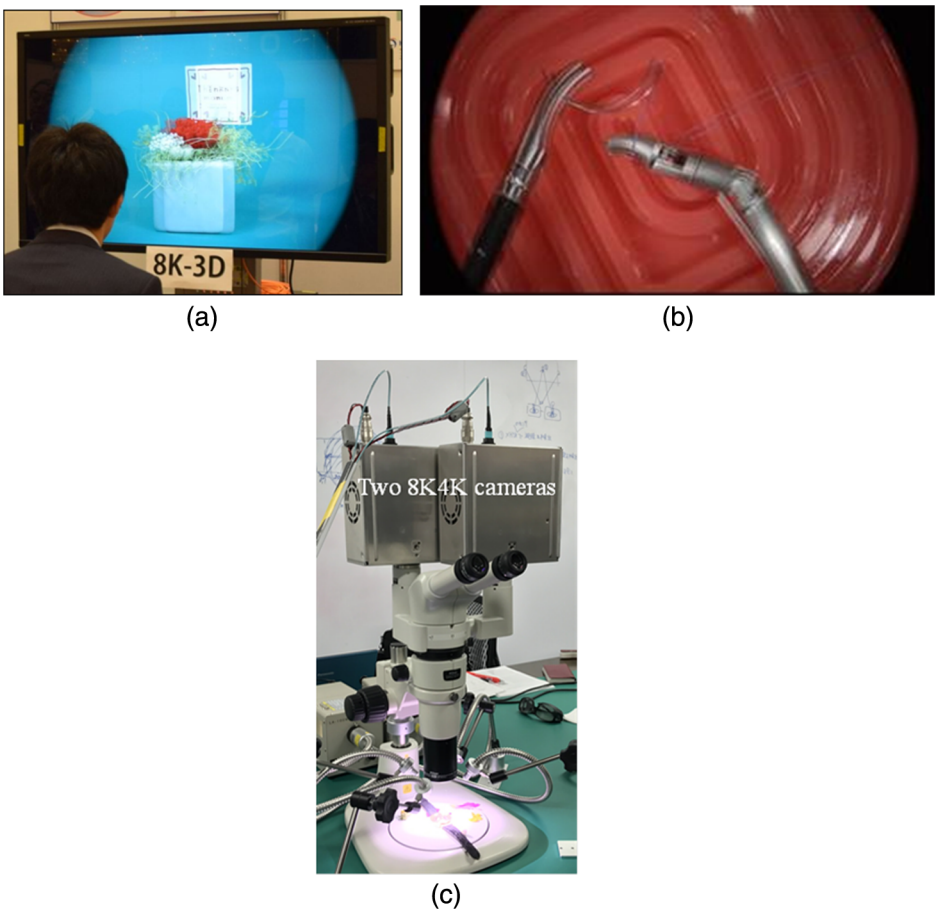

Fig. 25 The 8K-3D LCD (a) demonstration of 8K-3D, (b) example of 8K-3D images, and (c) a binocular stereoscopic microscope with two 8K4K cameras.

that the image quality of stereoscopic can be estimated before manufacturing.

3.4 *Image Quality*

First, we demonstrated the stereoscopic image on the 8K-3D LCD panel to ~50 people including surgeons, persons from medical-equipment- and video-equipment-suppliers, and interviewed them for the efficacy and impressions about the image quality. We displayed 3-D computer graphics (CG) for demonstrations. The CG, which was constructed 3-D model data such as laser scanned skeleton specimens and 1 million polygons, was rendered at 8K4K resolution. Observers made some comments that "pixels cannot be seen at all," "it seems to be natural, and the eyes do not get tired," and "real things are in front of me." Next, we had several demonstrations at various medical conferences and exhibitions using real 3-D images taken with 8K4K camera as shown in Fig. 25(a). As a result, we obtained a high rating about the image quality.

An example of 8K-3D images shown in Fig. 25(b) is the situation when we tried sutures with endoscopic surgical instruments. First, we took this image using two 8K4K cameras simultaneously, which were developed by JVCKENWOOD Corporation and Kairos Co., Ltd., mounted on a binocular stereoscopic microscope (Nikon Corporation, SMZ1270 and Plan Apo 0.5x/WF objective lens) for the first experimental model of an 8K-3D medical microscope in the world as shown in Fig. 25(c), after that converted to the 3-D image format for the space division technique. These 3-D images on the 8K-3D LCD provide the sense of depth and reality for observers. From now on, we are planning to evaluate the clinical application of the 8K-3D system with this IPS-LCD, such as an 8K-3D medical endoscope/microscope.

4 Conclusion

We have developed a 55-inch 8K4K IPS-LCD with a high frame frequency of 120 Hz and with wide color gamut on the basis of a laser backlight system. Moreover, stereoscopic has been possible. The APD, developed as a unique technology, enabled to operate at 120 Hz, regardless of the backplane based on an a-Si technology. Remarkably, the achievement of a high resolution of 8K4K and a high frame frequency of 120 Hz is the World's first for LCDs with a-Si backplanes. Furthermore, the color gamut is expands far wider owing to a backlight system with laser light source. We developed the new LCD that can cover 99% of color space defined in BT.2020. In addition, we have established stereoscopic 8K4K technology. A 3-D polarization filter is attached on the 55-in. 8K4K LCD, which enables endoscopes and head-up surgeries having stereoscopic with high-quality image.

Acknowledgments

A part of this work was carried out as an entrustment of development from Kairos Co., Ltd., supported by Japan Agency for Medical Research and Development (AMED) grant "Developing smart treatment centers with balanced safety and enhanced medical efficiency (8K endoscope systems)." Moreover, the authors are grateful to Nikon Corporation for technical assistance with the experiment to record 8K-3D microscopic images.

References

1. Ministry of Internal Affairs and Communications, Japan, White Paper 2016, Chapter 6 ICT Policy Directions, Section 4 Developments in Broadcasting Policy, http://www.soumu.go.jp/johotsusintokei/whitepaper/eng/WP2016/chapter-6.pdf#page=4 (2016).
2. Recommendation ITU-R BT.2020, "Parameter values for ultra-high definition television systems for production and international programme exchange," https://www.itu.int/dms_pubrec/itu-r/rec/bt/R-REC-BT.2020-2-201510-I!!PDF-E.pdf (2015).
3. H. Yamashita et al., "Ultra-high definition (8K UHD) endoscope: our first clinical success," *SpringerPlus* **5**, 1445 (2016).
4. T. Nakamura, "Research and development towards practical-use full-featured 8k super hi-vision cameras," Science & Technical Research Laboratories R&D, No. 164 (2017).
5. T. Sakiyama et al., "8K-UHDTV production equipment and workflow which realize an unprecedented video experience," in *SMPTE 2016 Annual Technical Conf. and Exhibition*, pp. 1–11 (2016).
6. S. Namiki et al., "Ultrahigh-definition video transmission and extremely green optical networks for future," *IEEE J. Sel. Top. Quantum Electron.* **17**(2), 446–457 (2011).
7. Y. Sugito et al., "Development of HEVC/H.265 Codec system and transmission experiments aimed at 8k broadcasting," Science & Technical Research Laboratories R&D, No. 155 (2016).
8. Sharp Corporation, "Sharp announces release of AQUOS 8K in Japan, China, Taiwan, and Europe—World's First 8K-compatible TVs and displays bring on-screen reality closer than ever," Press Releases, http://www.sharp-world.com/corporate/news/170831.html (2017).
9. Y. Mishima et al., "Development of a 19-in.-diagonal UXGA super TFT-LCM applied with super-IPS technology," in *SID Symp. Digest of Technical Papers*, Vol. 31, pp. 260–263 (2000).
10. J. Maruyama et al., "55-inch 8K4K IPS-LCDs with high frame frequency, wide color gamut and stereovision," *Proc. SPIE* **10557**, 105570S (2018).
11. S. H. Lee et al., "'18.1' Ultra-FFS TFT-LCD with super image quality and fast response time," in *SID Symp. Digest of Technical Papers*, Vol. 32, pp. 484–487 (2001).
12. K. Ono et al., "New IPS technology suitable for LCD-TVs," in *SID Symp. Digest of Technical Papers*, Vol. 36, pp. 1848–1851 (2005).
13. K. Ono et al., "Improvement of motion blur for IPS-Pro LCD-TVs driven by 180 Hz impulsive driving," in *SID Symp. Digest of Technical Papers*, Vol. 36, pp. 1954–1957, (2006).
14. K. Ono and I. Hiyama, "The latest IPS pixel structure suitable for high resolution LCDs," in *Proc. Int. Display Workshops*, pp. 933–936 (2012).
15. R. Oke et al., "An application of new TFT driving method for 47-in. diagonal IPS LCDs with resolutions of QFHD and FHD," in *Proc. Int. Display Workshops*, pp. 945–948 (2012).
16. K. Endo, R. Oke, and K. Ono, "Column line driving for IPS-Pro LCD-TVs," in *Proc. Int. Display Workshops*, pp. 255–256 (2006).
17. R. Oke et al., "World's first 55-in. 120 Hz-driven 8K4K IPS-LCDs with wide color Gamut," in *SID Symp. Digest of Technical Papers*, pp. 1055–1058 (2015).
18. I. Hiyama et al., "The latest IPS-LCD technology realizing super high resolution and wide color Gamut," in *Proc. Int. Display Workshops*, pp. 9–11 (2015).
19. Y. Koike and A. Inoue, "High-speed graded-index plastic optical fibers and their simple interconnects for 4K/8K video transmission," *IEEE J. Lightwave Technol.* **34**, 1551–1555 (2016).
20. T. Tanabe et al., "Circularly polarized (CPL) 3D monitors attract attention again for medical applications," in *SID Symp. Digest of Technical Papers*, pp. 987–990 (2015).

Ryutaro Oke is a chief engineer at Panasonic Liquid Crystal Display Co., Ltd. He received his BE and ME degrees in electronic engineering from Nagoya University in 1997 and 1999, respectively. He has been engaged in the development of LCDs, and he was a project leader who led to success of this 8K4K panel. He received the Commendation for Science and Technology by the Minister of Education, Culture, Sports, Science and Technology in Japan in 2015.

Junichi Maruyama is an engineer at Panasonic Liquid Crystal Display Co., Ltd., and a specialist of display systems. He received his master's degree in engineering from Tokyo Institute of Technology in 2000. He made a big contribution to the development of this 8K-LCD systems. He received the best paper award at the 24th International Display Workshops in 2017.

Tomohiro Murakoso is a manager at Panasonic Liquid Crystal Display Co., Ltd. He received his BE and MS degrees in electronic engineering from Tokyo Institute of Technology in 1998 and 2000, respectively. He joined Matsushita Electric Industrial Co., Ltd., where he engaged in research and development of plasma displays. He moved to Panasonic Liquid Crystal Display Co., Ltd. in 2014, where he continues to work in the design and the development of IPS TFT-LCDs.

Masahiro Ishii is a chief engineer at Panasonic Liquid Crystal Display Co., Ltd. He received his BE and MS degrees in electronic engineering from Kyoto University in 1991 and 1993, respectively. He joined Hitachi Research Laboratory, Hitachi, Ltd., where he engaged in R&D of LCDs. He moved to IPSα Technology, Inc. in 2008, which subsequently changed to Panasonic Liquid Crystal Display Co., Ltd. in 2010, where he continues to work in the development of IPS TFT-LCDs.

Ikuo Hiyama is a general manager at Panasonic Liquid Crystal Display Co., Ltd. He received his BE and MS degrees in electronic engineering from Keio University in 1988 and 1990, respectively. He joined Hitachi Research Laboratory, Hitachi, Ltd. where he engaged in R&D of LCDs. He moved to IPSα Technology, Inc. in 2008, which subsequently changed to Panasonic Liquid Crystal Display Co., Ltd. in 2010, where he continues to work in the development of IPS TFT-LCDs.

Yoshihisa Kato received his BS and MS degrees in electrical engineering from Osaka University and a doctoral degree in material science from Nara Institute of Science and Technology in 1987, 1989, and 2009, respectively. He joined Panasonic Corporation in 1989 and was engaged in research and development of LCDs. Since 2000, he has studied ferroelectric random access memories and image sensors. His current interest is focused on enhancement of the contrast ratio of LCDs.

Hiromasa Yamashita received his PhD from Graduate School of Information Science and Technology, The University of Tokyo. He is a research resident, National Center for Child Health and Development (NCCHD). He is an assistant professor, The University of Tokyo in 2008. He is a research fellow for NCCHD in 2010. He is the director for Medical Imaging Consortium in 2012. He is an associate professor of University Research Center, Nihon University in 2015. He is the board director, Kairos Co., Ltd. in 2017. His research interests include medical imaging, robotics and navigation systems, and mechanical engineering.

Kenkichi Tanioka joined the NHK Kochi. He received his PhD in 1976, he transferred to the NHK Science & Technology Research Laboratories (NHK STRL) and researched and developed amorphous selenium photoconductive film for image sensors. In 2006, he is the director-general, NHK STRL. In 2012, he is the vice president, Medical Imaging Consortium. In 2016, he is the technical advisor, Kairos Co., Ltd. In 2017, he is a research professor, The State University of New York at Stony Brook. He is the fellow and honorary member, The Institute of Image Information and Television Engineers.

Toshio Chiba graduated Tohoku University School of Medicine. He received his MD and PhD degrees. His specialties are fetal surgery and pediatric surgery. In 1986, he is a visiting assistant professor/clinical fellow, Division of Pediatric Surgery, University of Pittsburgh. In 1998, he is a visiting professor, The Fetal Treatment Center, UCSF. In 2001, he is the director, Department of Strategic Medicine, National Center for Child Health and Development. In 2012, he is the chairman, Medical Imaging Consortium. In 2013, he is a professor, The University of Tokyo. In 2015, he is a professor, Nihon University. In 2016, he is the CEO Kairos Co., Ltd.